

Formation of Highly Ordered Self-Assembled Monolayers of Alkynes on Au(111) Substrate

Tomasz Zaba,[‡] Agnieszka Noworolska,[‡] Carleen Morris Bowers,[§] Benjamin Breiten,[§] George M. Whitesides,[§] and Piotr Cyganik^{*‡}

[‡]Smoluchowski Institute of Physics, Jagiellonian University, ul. Reymonta 4, 30-059 Krakow, Poland

[§]Department of Chemistry and Chemical Biology, Harvard University, 12 Oxford Street, Cambridge, Massachusetts 02138, United States

S Supporting Information

ABSTRACT: Self-assembled monolayers (SAMs), prepared by reaction of terminal *n*-alkynes ($\text{HC}\equiv\text{C}(\text{CH}_2)_n\text{CH}_3$, $n = 5, 7, 9,$ and 11) with Au(111) at 60°C were characterized using scanning tunneling microscopy (STM), infrared reflection absorption spectroscopy (IRRAS), X-ray photoelectron spectroscopy (XPS), and contact angles of water. In contrast to previous spectroscopic studies of this type of SAMs, these combined microscopic and spectroscopic experiments confirm formation of highly ordered SAMs having packing densities and molecular chain orientations very similar to those of alkanethiolates on Au(111). Physical properties, hydrophobicity, high surface order, and packing density, also suggest that SAMs of alkynes are similar to SAMs of alkanethiols. The formation of high-quality SAMs from alkynes requires careful preparation and manipulation of reactants in an oxygen-free environment; trace quantities of O_2 lead to oxidized contaminants and disordered surface films. The oxidation process occurs during formation of the SAM by oxidation of the $-\text{C}\equiv\text{C}-$ group (most likely catalyzed by the gold substrate in the presence of O_2).

Thin organic films based on self-assembled monolayers (SAMs)¹ are ubiquitous in surface science. The reaction of organic thiols (RSH) with group Ib metals (Au and Ag) to generate SAMs with composition Au/AgSR is the reaction most commonly used to prepare SAMs,¹ although reactions that generate organosilanes on silicon² (SiR) and organic carboxylates on silver³ (AgO_2CR) have attractive properties, and a number of other precursors have been surveyed. There have also been scattered descriptions of SAMs formed on gold from solutions of alkynes⁴ ($\text{HC}\equiv\text{C}(\text{CH}_2)_n\text{CH}_3$, $n = 3, 5, 7, 9, 11,$ and 13), ethynylbenzene⁵ ($\text{HC}\equiv\text{CC}_6\text{H}_5$) or *n*-alkylmercury(II) tosylates⁶ ($\text{CH}_3(\text{CH}_2)_n\text{HgOTs}$, $n = 4$ and 18) on Au(111). Although the potential interest of SAMs having metal– $\text{C}\equiv\text{CR}$ bonds is high, since they offer a new type of metal–organic bond, most of these studies have used preparations analogous to those employed with *n*-alkanethiols and have generated SAMs that do not seem to be highly ordered and, thus, are perhaps unsuitable for detailed studies of the physical chemistry of the surface. In particular, there are no procedures that describe the formation of SAMs that are highly

ordered in two dimensions—a key requirement for high-quality surface science. The most recent analyses of *n*-alkyl-based SAMs on Au(111) indicate a “liquid-like” structure of the monolayer,⁶ and XPS analyses of SAMs formed from alkynes^{4,5} suggest that these SAMs are sensitive to oxidation at an undefined point in their formation; that is, oxidation occurs either during or after SAM formation (for example, by reaction of the $\text{AuC}\equiv\text{CR}$ bond with O_2). Contact angle analyses of increasing lengths of alkynes ($\text{HC}\equiv\text{C}(\text{CH}_2)_n\text{CH}_3$, $n = 5, 7, 9,$ and 11) also suggest⁴ that the quality of these SAMs is lower than those based on *n*-alkanethiols.

Although SAMs have enabled studies of wetting,^{7,8} adhesion,^{9,10} and charge transport^{3,11–13} (inter alia), most of this work has focused on the terminal part of the SAM that is exposed to air, and there is relatively little work devoted to understanding the contribution of the anchoring groups of the SAM (as opposed to the terminal group, the thickness, or the electronic structure). Herein, we characterize the SAMs formed by reactions of *n*-alkynes ($\text{HC}\equiv\text{C}(\text{CH}_2)_n\text{CH}_3$, $n = 5, 7, 9,$ and 11) with Au(111). We believe that the $\text{AuC}\equiv\text{CR}$ group is particularly interesting as the basis for SAMs on Au for two reasons: (i) the acetylene group connects with Au atoms on the surface by a strong σ -bond;¹⁴ (ii) the orbital structure of the acetylene group and the existence of a variety of stable organometallic compounds containing the $\text{AuC}\equiv\text{CR}$ group suggest that the interface between the metal, Au, and the saturated organic component of the SAM ($\text{R} = (\text{CH}_2)_n\text{CH}_3$), might be informative in studies in which the interface connecting the SAM to the metallic substrate might contribute to its properties.

The objective of this work is to study the order of *n*-alkyne-derived SAMs on gold through a combination of microscopic, spectroscopic, and contact angle measurements. Our results show that the disorder and mixed organic functionality implied by previous work^{4–6} are artifacts reflecting oxidation of the terminal acetylene by O_2 in solution during formation of the SAM (perhaps in a reaction catalyzed by Au),¹⁵ and that using appropriate experimental conditions (e.g., rigorous exclusion of O_2 , a slightly elevated temperature of 60°C during formation of the SAM) results in well-organized SAMs of alkynes that have qualities similar to those of alkanethiols on Au(111).

Received: July 2, 2014

Published: August 7, 2014

These studies thus establish that SAMs of the surface composition $\text{AuC}\equiv\text{CR}$ provide a new type of SAM for use in physical and physical-organic studies having an interface to gold, and are complementary to the well-understood SAMs of alkanethiols (AuSR).

SAMs of alkynes were prepared on Au by submerging freshly evaporated Au(111) substrates in a 1 mM ethanolic solution of *n*-alkyne ($\text{HC}\equiv\text{C}(\text{CH}_2)_n\text{CH}_3$, $n = 5, 7, 9$, and 11) for 15 h at 60 °C. Importantly, the preparation of the SAMs was performed in an O_2 -free environment to avoid oxidation of the acetylene group. The Supporting Information (SI) provides a more detailed description of the experimental procedure, as well as additional details of measurements.

Figure 1 summarizes results obtained by scanning tunneling microscopy (STM) for decyne ($n = 7$) chemisorbed on Au(111). Larger-scale analysis (Figure 1a) shows formation of depressions on the substrate with depths compatible with substrate lattice steps due to a single layer of Au atoms (as indicated by the respective cross-section, marked by A). Such

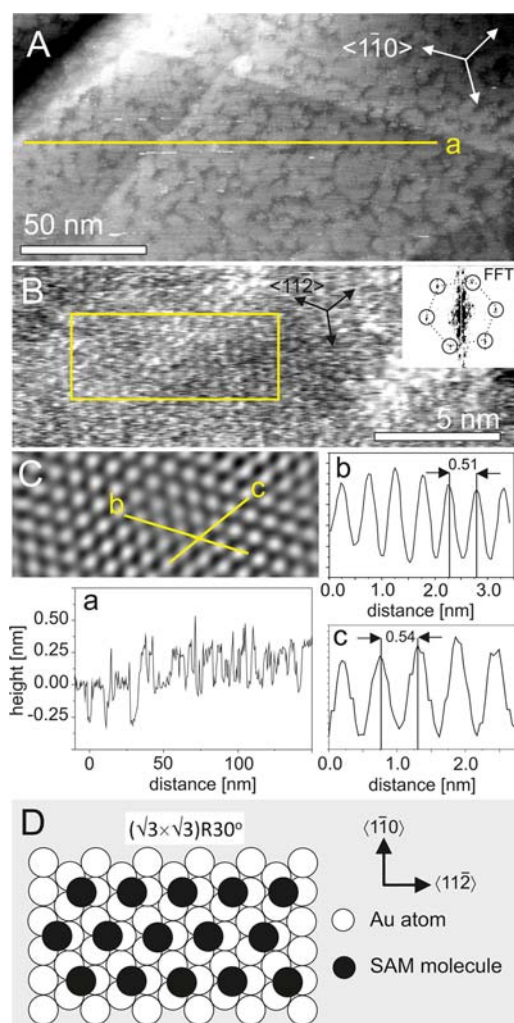


Figure 1. (A–C) STM data for decyne/Au(111) SAMs. Panels a, b, and c show cross sections a, b, and c indicated in (A–C), respectively. Inset in (B) shows FFT spectrum of image (B) with indicated 6-fold symmetry pattern. Yellow rectangle in (B) marks an area corresponding to the image shown in (C) obtained after FFT filtering of (B). (D) Scheme of decyne adsorption in the $(\sqrt{3} \times \sqrt{3})R30^\circ$ structure with arbitrarily taken adsorption seats.

depressions are also characteristic of formation of both thiol¹ and selenol¹⁶ based SAMs on Au(111), and likely result mainly from lifting the Au(111) herringbone reconstruction upon chemisorption of these molecules.¹⁷ Detection of similar features for alkynes suggests formation of densely packed chemisorbed structures on Au(111).

This inference of a dense monolayer is confirmed by high-resolution STM, accompanied by Fourier analysis (using fast Fourier transform, FFT), which shows a hexagonal lattice. The data obtained after FFT filtering (Figure 1c) suggest a hexagonal structure with a period of 5 Å, as indicated by the line scans along the axes. The structure inferred from this analysis (shown schematically in Figure 1d) is consistent with the $(\sqrt{3} \times \sqrt{3})R30^\circ$ lattice (which characterizes the structure formed by alkanethiols on Au(111)¹⁸ and leads to an area per molecule of 21.5 Å²). While the quality of our data does not permit a more detailed description of the structure (as was possible for alkanethiols, which exhibit a $c(4 \times 2)$ superlattice),¹⁸ it certainly shows that alkynes on Au(111) form well-ordered structures with packing densities similar to those of alkanethiols (area per molecule 21.5 Å²).

To characterize the orientational order of alkyne-based SAMs further, we used infrared reflection absorption spectroscopy (IRRAS). IRRAS measurements of the SAMs—formed by reaction of octyne ($n = 5$), decyne ($n = 7$), dodecyne ($n = 9$), and tetradecyne ($n = 11$) with Au(111)—showed vibrational bands in the C–H stretching range at 2965 cm^{-1} (aCH_3), 2938 cm^{-1} (sCH_3, FR), 2920 cm^{-1} (aCH_2), 2878 cm^{-1} (sCH_3, FR), and 2851 cm^{-1} (sCH_2) (Figure 2). For

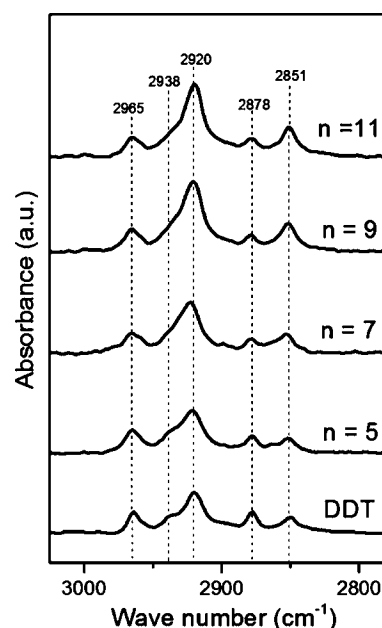


Figure 2. Overview of IRRAS data for $n = 5, 7, 9$, and 11 alkynes on Au(111) together with the corresponding DDT/Au(111) in the characteristic C–H stretching range.

comparison, analogous IRRAS measurements were performed on SAMs of dodecanethiol (DDT) on Au(111). This comparison shows that the frequencies, relative intensities, and the bandwidth of the spectra for $\text{AuC}\equiv\text{CR}$ and AuSR are similar (for more details see Figure 1S in the SI).¹⁹ For the same orientation of *n*-alkynyl and alkanethiol on Au(111), however, we would expect the DDT ($n_{\text{CH}_2} = 11$) spectrum to

be close to that of tetradecyne ($n_{\text{CH}_2} = 11$), which has a comparable aliphatic chain length ($(\text{CH}_2)_n\text{CH}_3$). Instead, the DDT spectrum intensity is similar to that of octyne ($n_{\text{CH}_2} = 5$). As a result of surface selection rules, IRRAS intensities are sensitive to the orientation of the molecules within the SAM (with respect to the metal substrate). The data in Figure 2 show significant differences in the CH_2 bands, but similarities in the CH_3 bands; this result suggests, according to previous reports on IRRAS data,^{19,20} differences in the tilt angle and similarities in the twist angle of the $(\text{CH}_2)_n\text{CH}_3$ chain for the n -alkynyl and alkanethiolate on Au(111). Such differences are not surprising, considering the different bonding geometries for each SAM.

Figure 3 shows a more detailed analysis of the IRRAS spectra for tetradecyne, including a fitting for the C–H stretching

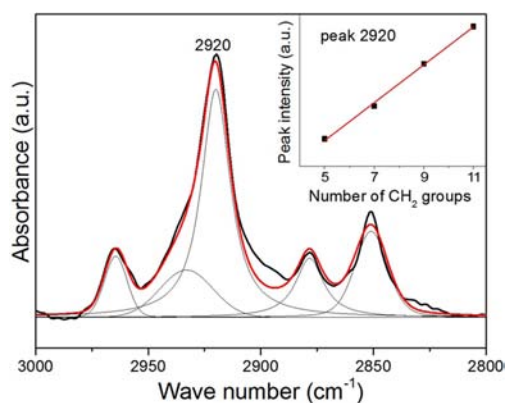


Figure 3. IRRAS data analysis for tetradecyne/Au(111) with fitting individual bands. Inset shows linear increase in 2920 cm^{-1} peak intensity as a function of the CH_2 group number.

modes. The inset in Figure 3 shows that an increase in the length of the aliphatic chain (from $n = 5$ up to $n = 11$) correlates linearly with the intensity of the CH_2 -related symmetric (2920 cm^{-1}) mode. This observation indicates that the conformation of n -alkynes on Au(111) is preserved across the entire series of alkynes that we investigated; Nuzzo et al. reported a similar observation in earlier spectroscopic studies of alkanethiols on Au.²⁰ In contrast to our observations, recent PM-IRRAS experiments by Scholz et al.⁶ (based on analysis of the C–H stretching range) performed for alkyl-based SAMs (n -butylmercury tosylate ($\text{C}_4\text{H}_9\text{HgOTs}$) and n -octadecylmercury tosylate ($\text{C}_{18}\text{H}_{37}\text{HgOTs}$) on Au) demonstrated fundamental differences in the relative intensities and band broadening between these SAMs and analogous alkanethiols; that is, the n -alkyls had a liquid-like structure (in contrast to the crystalline structure observed for n -alkanethiols). In contrast, the IRRAS data presented in Figures 2 and 3 demonstrate that it is possible to form alkynes that have order similar to that of alkanethiols on Au(111).

Figure 4 shows X-ray photoelectron spectroscopy (XPS) analysis of the alkyne-based SAMs. In contrast to previously reported XPS data for increasing lengths of alkynes ($\text{HC}\equiv\text{C}(\text{CH}_2)_n\text{CH}_3$, $n = 5, 7, 9, \text{ and } 11$),⁴ the C 1s signal in Figure 4 shows a single symmetric peak at 285 eV, with no additional higher-energy components (e.g., peaks at 287, 289 eV). The C 1s spectra are also consistent with the corresponding data obtained for DDT (Figure 4) as well as other literature data²¹ for unoxidized alkanethiols on Au(111). We calculated the film thickness using the C 1s/Au 4f intensity ratios (assuming an exponential attenuation of the photoelectron signal²² and using

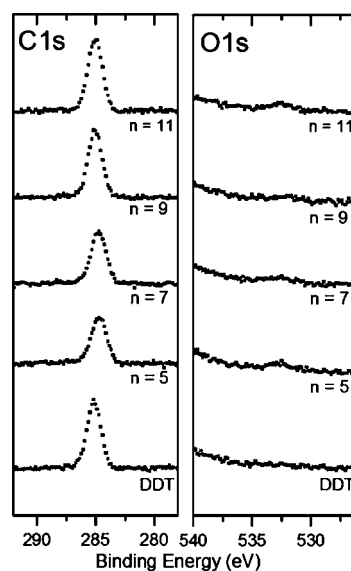


Figure 4. XPS C 1s and O 1s data for $n = 5, 7, 9, \text{ and } 11$ alkynes on Au(111) together with the corresponding DDT/Au(111).

attenuation lengths reported²³ earlier). The calculated values (see Figure 5) show a linear increase in thickness as a result of

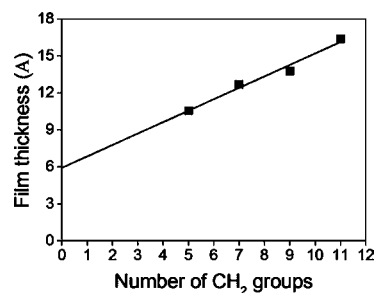


Figure 5. Film thickness calculated in number of methylene groups ($(\text{CH}_2)_n$) from the XPS data (see text) for SAMs of $\text{HC}\equiv\text{C}(\text{CH}_2)_n\text{CH}_3$, ($n = 5, 7, 9, \text{ and } 11$) on Au(111). The solid line indicates a linear fit.

an increase in the length of the chain (from $n = 5$ to $n = 11$). Importantly, the XPS data are consistent with the IRRAS data shown in Figure 3; they indicate a linear increase in the IR signal with an increasing number of methylene units (CH_2). Moreover, using the linear relation obtained from our XPS data, we can extrapolate the thickness of the film for $n = 0$ to a value of 5.9 Å ; this value corresponds to the length expected for a $-\text{C}\equiv\text{CCH}_3$ fragment. This extrapolation is also consistent with the 5.6 Å dimensions of an upright configuration of the $-\text{C}\equiv\text{CCH}_3$ molecule on Au(111), on the basis of the bonds lengths provided by previous DFT²⁴ calculations. Thus, the estimation of thickness using XPS is consistent with SAMs of $\text{HC}\equiv\text{C}(\text{CH}_2)_n\text{CH}_3$ on Au(111) having the $-\text{C}\equiv\text{C}-$ group perpendicular to the surface.¹⁴

Previously reported XPS data for SAMs derived from ethynylbenzene ($\text{HC}\equiv\text{CC}_6\text{H}_5$) on Au⁵ suggested that the SAM contained oxidized components, as is inferred from both a significant O 1s signal and higher-energy contributors to the C 1s peak (e.g., peaks at 287, 289 eV). In contrast, data shown in Figure 4 show only small traces of O 1s (the O 1s/C 1s signal ratio is <0.06) for all SAMs analyzed, which were prepared carefully in an O_2 -free environment (the SI details the

procedure). The oxidation of alkynes is indeed clearly visible for samples that were exposed to O₂ (ambient conditions) during preparation of the SAMs (see Figure 6). In the XPS data

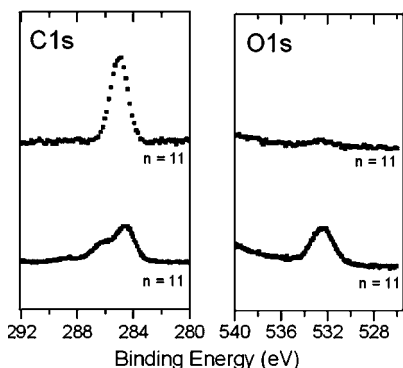


Figure 6. XPS region scans (C 1s and O 1s) for SAMs of HC≡C(CH₂)₁₁CH₃ on Au(111) prepared in an O₂-free atmosphere (upper spectra) and an O₂-containing atmosphere (lower spectra).

(Figure 6), an intense O 1s signal (O 1s/C 1s ratio = 0.92) in this case is associated with significant changes in the C 1s peak, and the appearance of higher-energy components (289, 287 eV) which cause significant asymmetry and broadening of the C 1s peak, and are indicative of the oxidation of the $-C\equiv C-$ group as reported in ref 5. Our data demonstrate that the oxidation of alkynes does not involve the C–Au(111) bond formation (as had been suggested previously⁵) but instead involves oxidation of the alkynes in solution during formation of the SAM.

The interfacial free energy of *n*-alkyl SAMs on Au(111) was investigated using measurements of advancing contact angles of water ($\Theta^a_{H_2O}$). The data (see Table 1 in the SI) are in a range ($\Theta^a_{H_2O} = 111^\circ$ – 115°) that is consistent with the values measured here for DDT/Au(111), as well as literature data²⁵ for SAMs of alkanethiols on Au(111). The values of $\Theta^a_{H_2O}$ presented here are significantly higher than those reported previously (89° – 98°) for alkynes on Au(111),⁴ and serve as additional evidence of a similar degree of order for SAMs of alkynes (prepared properly) and alkanethiols on Au(111).

In conclusion, our STM and IRRAS data show that alkynes on Au(111) form SAMs that have organization and structure similar to alkanethiols on Au(111). High surface ordering and packing density of alkynes is also consistent with high values of $\Theta^a_{H_2O}$. The XPS data show that the presence of oxygen marks contamination of alkyne-based SAMs through oxidation of the acetylene group. The oxidation of $-C\equiv C-$ (most likely catalyzed by the gold substrate in the presence of O₂) can be monitored by the appearance of high-energy components and a broadening and asymmetry in the C 1s signal. Alkynes appear to be more sensitive to oxidation than alkanethiols during formation of the SAM and require the formation to be carried out carefully in an O₂-free atmosphere.

■ ASSOCIATED CONTENT

Supporting Information

Experimental details. This material is available free of charge via the Internet at <http://pubs.acs.org>.

■ AUTHOR INFORMATION

Corresponding Author

piotr.cyganik@uj.edu.pl

Notes

The authors declare no competing financial interest.

■ ACKNOWLEDGMENTS

We thank Prof. Marek Szymanski for providing access to the STM microscope at the Department of Physics of Nanostructures and Nanotechnology at the Jagiellonian University. We would like to thank Andreas Roetheli for helpful discussions concerning the oxidation of acetylenes. This work was supported financially by the National Science Centre Poland (Grant DEC-2013/10/E/ST5/00060). The XPS equipment was purchased with the financial support of the European Regional Development Fund (Grant POIG.02.01.00-12-023/08). The work at Harvard University was supported by a subcontract from Northwestern University from the United States Department of Energy (DOE, DE-SC0000989).

■ REFERENCES

- (1) Love, J. C.; Estroff, L. A.; Kriebel, J. K.; Nuzzo, R. G.; Whitesides, G. M. *Chem. Rev.* **2005**, *105*, 1103.
- (2) Li, Y.; Calder, S.; Yaffe, O.; Cahen, D.; Haick, H.; Kronik, L.; Zuilhof, H. *Langmuir* **2012**, *28*, 9920.
- (3) Liao, H. C.; Yoon, H. J.; Bowers, C. M.; Simeone, F. C.; Whitesides, G. M. *Angew. Chem., Int. Ed.* **2014**, *53*, 3889.
- (4) Zhang, S.; Chandra, K. L.; Gorman, C. B. *J. Am. Chem. Soc.* **2007**, *129*, 4876.
- (5) McDonagh, A. M.; Zareie, H. M.; Ford, M. J.; Barton, C. S.; Ginic-Markovic, M.; Matisons, J. G. *J. Am. Chem. Soc.* **2007**, *129*, 3533.
- (6) Scholz, F.; Kaletova, E.; Stensrud, E. S.; Ford, W. E.; Kohutova, A.; Mucha, M.; Stibor, I.; Michl, J.; Wrochem, F. *J. Phys. Chem. Lett.* **2013**, *4*, 2624–2629.
- (7) Drelich, J.; Wilbur, J. L.; Miller, J. D.; Whitesides, G. M. *Langmuir* **1996**, *12*, 1913.
- (8) Hao, Y. J.; Soolaman, D. M.; Yu, H. Z. *J. Phys. Chem. C* **2013**, *117*, 7736.
- (9) Vezenov, D. V.; Zhuk, A. V.; Whitesides, G. M.; Lieber, C. M. *J. Am. Chem. Soc.* **2002**, *124*, 10578.
- (10) Khan, M. N.; Tjong, V.; Chilkoti, A.; Zharnikov, M. *Angew. Chem., Int. Ed.* **2012**, *51*, 10303.
- (11) Holmlin, R. E.; Haag, R.; Chabynec, M. L.; Ismagilov, R. F.; Cohen, A. E.; Terfort, A.; Rampi, M. A.; Whitesides, G. M. *J. Am. Chem. Soc.* **2001**, *123*, 5075.
- (12) Venkataraman, L.; Klare, J. E.; Nuckolls, C.; Hybertsen, M. S.; Steigerwald, M. L. *Nature* **2006**, *442*, 904.
- (13) McCreery, R. L.; Bergren, A. J. *Adv. Mater.* **2009**, *21*, 4303.
- (14) Maity, P.; Takano, S.; Yamazoe, S.; Wakabayashi, T.; Tskuda, T. *J. Am. Chem. Soc.* **2013**, *135*, 9450.
- (15) Tkatchouk, E.; Goddard, W. A.; Toste, D.; Brenzovich, W. E.; Lackner, A. D.; Shunatona, H. P.; Benitez, D. *Abstr. Pap. Am. Chem. Soc.* **2011**, *241*, 136.
- (16) Romashov, L. V.; Ananikov, V. P. *Chem.—Eur. J.* **2013**, *19*, 17640.
- (17) Poirier, G. E. *Langmuir* **1997**, *13*, 2019.
- (18) Poirier, G. E. *Chem. Rev.* **1997**, *97*, 1117.
- (19) Debe, M. K. *J. Appl. Phys.* **1984**, *55*, 3345.
- (20) Laibinis, P. E.; Whitesides, G. M.; Allara, D. L.; Tao, Y. T.; Parikh, A. N.; Nuzzo, R. G. *J. Am. Chem. Soc.* **1991**, *113*, 7152.
- (21) Zharnikov, M.; Geyer, W.; Golzhauser, A.; Frey, S.; Grunze, M. *Phys. Chem. Chem. Phys.* **2000**, *1*, 3163.
- (22) Dannenberger, O.; Weiss, K.; Himmel, H. J.; Jager, B.; Buck, M.; Woll, C. *Thin Solid Films* **1997**, *307*, 183.
- (23) Lamont, C. L. A.; Wilkes, J. *Langmuir* **1999**, *15*, 2037.
- (24) Ford, M. J.; Hoft, R. C.; McDonagh, A. M. *J. Phys. Chem. B* **2005**, *109*, 20387.
- (25) Bain, C. D.; Troughton, E. B.; Tao, Y. T.; Evall, J.; Whitesides, G. M.; Nuzzo, R. G. *J. Am. Chem. Soc.* **1989**, *111*, 321.